PAPER

NJC
www.rsc.org/njc

Synthesis and interfacial properties of amphiphatic cryptophanes†

Isabelle Gosse,‡[a] Jean-Paul Chauvet[b] and Jean-Pierre Dutasta*[a]

[a] *Laboratoire de Chimie, UMR CNRS 5182, École Normale Supérieure de Lyon, 46 allée d'Italie, F-69364 Lyon 07, France. E-mail: dutasta@ens-lyon.fr; Fax: +33 4 7272 8483; Tel: +33 4 7272 8382*

[b] *IFoS-PCI, UMR CNRS 5621, Équipe Bioingénierie et Reconnaissance Génétique École Centrale de Lyon, 36 avenue Guy de Collongue, BP 163, F-69131 Ecully Cedex, France*

Received (in Montpellier, France) 6th July 2005, Accepted 22nd September 2005
First published as an Advance Article on the web 13th October 2005

The new amphiphatic cryptophanes **M5** and **M6** were synthesized from their precursor **M4**. They present interesting properties due to their long chain substituents on one of the cyclotriveratrylene moieties. **M4** was synthesized from a thio-cyclotriveratrylene platform obtained from thio-vanillin, using the template method developed for the preparation of dissymmetrical cryptophanes. The tris-hexanol (**M5**) or tris-hexadecyl (**M6**) substituted cryptophanes exhibited enhanced amphiphatic properties, which were investigated through the π–A isotherms of the interfacial films obtained at the air–water interface (Langmuir monolayers). The corresponding surface elasticity coefficients of the films were determined and their stability analyzed at different surface pressures. Stable molecular films of **M5** were obtained after a first compression step, suggesting a rearrangement of the molecules at the interface. This behavior matched with a reduction of the molecular area consistent with the formation of bilayers of **M5** molecules. Cryptophane **M6** formed stable and reversible Langmuir monolayers at higher surface pressure ($\pi_{max} = 27$ mN m^{-1}). This was attributed to interactions between the long alkyl chain substituents of the cryptophane, which favor the organization of the molecules on the water subphase. At higher pressure both compounds form aggregates irreversibly.

Introduction

Supramolecular systems forming stable self-assembling monolayers are conveniently used in the design of sensor devices, particularly in view of their potential applications as active materials for chemical recognition.[1] Traditionally, mono or multilayer systems obtained through an efficient deposition process are well adapted for this purpose. Increasing efforts in the search for new host molecules, which can produce organic thin films, are still unabated. They are focused on new strategies for producing amphiphatic organic receptors, and several categories of supramolecular systems have been explored such as modified cyclodextrins,[2] calixarenes[3] and resorcinarenes,[4] whose amphiphatic character was enhanced by adding functionalized hydrocarbon chains. They have been successfully assembled at the air–water interface or deposited on solid surfaces.[5] The cryptophanes represent another family of hollow molecules with a great ability to form stable inclusion complexes with a variety of neutral and cationic guest molecules.[6] Although they do not possess a conventional amphiphilic structure, they are good candidates for the construction of organized 2D assemblies. Indeed, it has been shown that they can form reversible monomolecular layers at the air–water interface, but with a rather limited stable surface pressure domain.[7] The behavior of these bowl-shaped molecules may be improved by introducing groups on their periphery, which can enhance their amphiphatic character and consequently lead to a significant improvement of the stability of the corresponding interfacial films.

This paper describes the synthesis of the new cryptophanes **M5** and **M6** from their common precursor cryptophane **M4**.[8] Their properties were investigated and compared to that of cryptophane **M**, which has no peripheral amphiphilic groups. **M4** possesses three ester functions, allowing the introduction of other functionalities by transesterification reactions. Two different substituents were thus introduced: three hexanol chains (**M5**) or three hexadecyl hydrocarbon chains (**M6**). The properties of the molecular films formed at the air–water interface were investigated by determining the surface pressure–molecular area isotherms (π–A), and by measuring the stability and the surface elasticity coefficient K_s. Finally, the organization of the molecules at the interface is discussed, according to the data reported herein.

Results and discussion

Synthesis

The synthesis of the precursor **M4** is outlined in Scheme 1, using the so-called template method, which normally produces the *anti* isomer with an excellent selectivity with respect to the *syn* isomer.[9] The triester-cyclotriveratrylene **1** was prepared in 7 steps from vanillin, according to previously reported methods.[10] The conversion of **1** to **2** was carried out by reaction with sodium isopropanethiolate in HMPA at 120 °C, followed by hydrolysis in concentrated sulfuric acid. The cyclotriveratrylene **2** was isolated in 46% yield. Reaction of vanillyl alcohol with 1,4-dibromobutane furnished the brominated derivative **3** following the literature procedure.[9] Reaction of **3** with dihydropyran in the presence of a catalytic amount of *p*-toluene sulfonic acid afforded the protected benzyl alcohol **4** in 95% yield. The next step is the condensation of **4** and cyclotriveratrylene **2** in presence of caesium fluoride in DMF. CsF is a very weak base allowing hydrogen bonding between fluoride

† Dedicated to the memory of Prof. Jean-Paul Chauvet, deceased on 12th January, 2003.
‡ Present address: Laboratoire d'Analyse Chimique par Reconnaissance Moléculaire, École Nationale Supérieure de Chimie et de Physique de Bordeaux, 16 Av. Pey Berland, 33607 Pessac, France.

DOI: 10.1039/b509291d

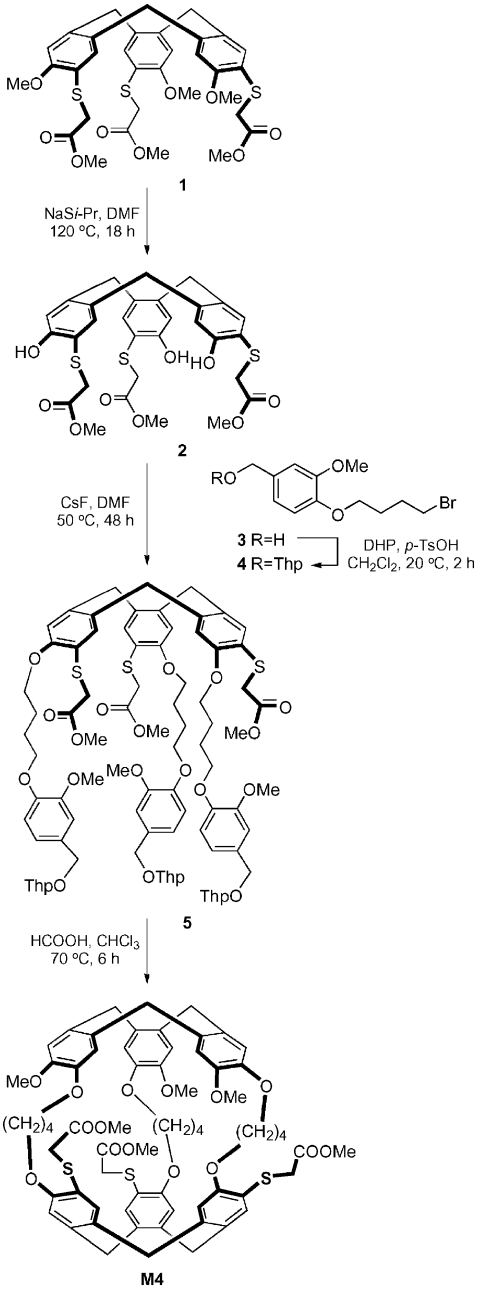

Scheme 1 Template synthesis of the triester-cryptophane **M4**.

and the OH groups in **2**.[11] This base has already been used in the alkylation of calixarenes to give the corresponding alkylated derivatives in high isolated yields.[12] The cyclotriveratrylene **5** was then obtained in 75% yield after column chromatography. When a strong base like NaOH was used, deprotonation on the α-position of the carbonyl occurred, and a non-separable mixture of by-products was thus obtained. In a similar synthesis using K_2CO_3 as base, no cyclotriveratrylene **5** was isolated. The last step is the intramolecular trimerization reaction of **5** in formic acid containing a small amount of $CHCl_3$ to give cryptophane **M4**, which was isolated by column chromatography in 29% yield. The FAB-MS of **M4** showed the expected molecular peak at *m*/*z* 1201.3.

The rather complicated proton NMR spectrum of **M4** did not allow proof of the *anti* structure of the molecule. However, a mixture of *syn* and *anti* isomers was not expected. As previously observed during the template synthesis of cryptophanes, the *anti* isomer is mainly obtained with the molecule possessing an even number of methylene groups in the linking chains.[6] In the present case, the *anti* configuration was assigned

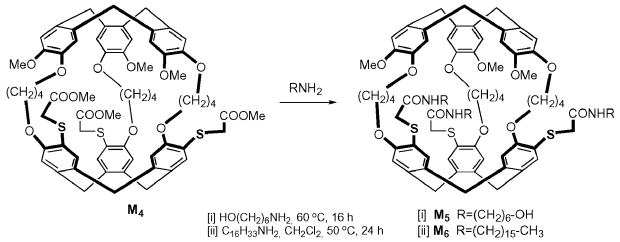

Scheme 2 Synthesis of amphiphatic cryptophanes **M5** and **M6**.

to the major compound obtained, although only an X-ray structure determination could ascertain this hypothesis. We note that chiral HPLC analysis would be inefficient, as both isomers are chiral (C_3 symmetry).

The preparation of the amphiphatic cryptophanes **M5** and **M6** was quite straightforward and is based on the reaction between the ester functions of cryptophane **M4** and a primary amine (Scheme 2).

Cryptophane **M5** was obtained by heating **M4** in melted 6-aminohexan-1-ol at 60 °C overnight under argon. **M5** was isolated by column chromatography in 75% yield. Similarly, **M6** was obtained when **M4** was stirred under argon in an excess of hexadecylamine at 50 °C for one day. The chromatographic separation afforded cryptophane **M6** in 55% yield. Mass spectra and NMR data were consistent with the **M5** and **M6** structures.

Interfacial films of cryptophanes

The specificity of cryptophanes **M5** and **M6** concerns the real domain of the monolayer, the molecular area extrapolated at zero pressure (defined in the experimental part), the behavior of the film after three compression–decompression cycles, the stability of the different films and the elasticity coefficient K_s. The K_s values for the cryptophane films can be compared to the values of the four typical 2D phases of fatty acids. According to the value of the K_s factor, four phases can be defined during the compression cycle: $K_s = 0$ mN m^{-1} defines a gas phase (G), $15 < K_s < 50$ mN m^{-1} defines an expanded liquid phase (EL), $100 < K_s < 250$ mN m^{-1} corresponds to a condensed liquid phase (CL) and $1000 < K_s < 2000$ mN m^{-1} characterizes a solid phase (S). The amphiphatic behavior at the air–water interface of the new cryptophanes **M5** and **M6** was compared to the interfacial properties of the parent compound **M**, which presents the same basic molecular structure without long chain substituents.

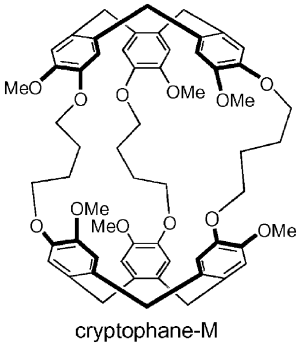

With compound **M**, isotherms were obtained in the whole range of compression, *i.e.* 2.20 to 0.50 nm^2 molecule^{-1}. For the first compression–decompression cycle, cryptophane **M** presents the typical π–*A* diagram of cryptophane derivatives (Fig. 1).[7a] The corresponding long-range isotherms are composed of three parts: two ascents of low compressibility (I and II) which are separated by a plateau. The existence of strong hysteresis, occurring during the decompression of the film, indicates that

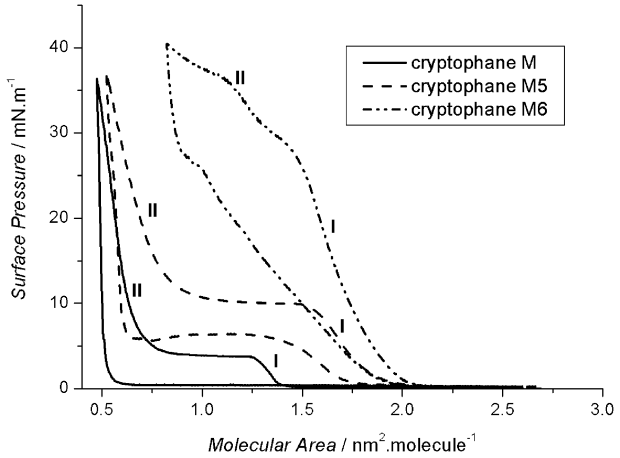

Fig. 1 π–A Isotherms for films of cryptophanes **M**, **M5** and **M6**.

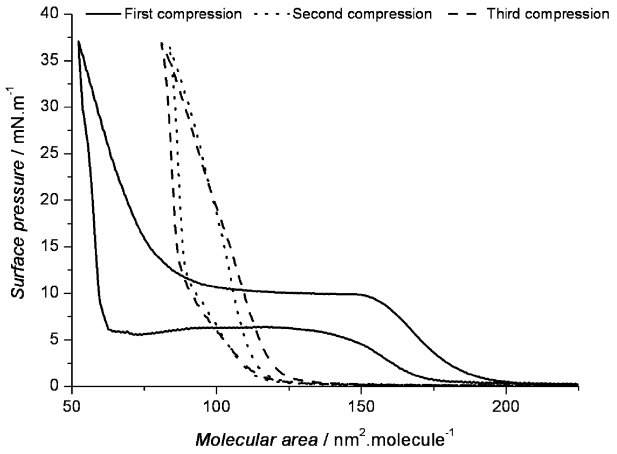

Fig. 2 Subsequent π–A isotherms for films of cryptophanes **M5**.

irreversible 3D aggregates or condensed 2D phases with a low dispersion process have been formed during the plateau and ascent (II) in the compression stage, as observed with other cryptophane molecules. It is thus obvious that the interfacial film of cryptophane **M** exists in a rather small range of surface pressure between 0 and 3.5 mN m^{-1}. Successive compression–decompression cycles did not show any modification of the behavior of the cryptophanes **M** assembly.

Isotherms determined with **M5** were also obtained in the whole range of compression (2.20 to 0.50 nm^2 $molecule^{-1}$). For the first compression–decompression cycle, cryptophanes **M** and **M5** behave similarly on the water surface (Fig. 1). The lift-off area is strongly increased by the presence of the chain substituents, from 1.4 to 2.0 nm^2 $molecule^{-1}$ for **M** and **M5** respectively. Due to the similar structure of the molecular cavity of both cryptophanes, this large difference is attributed to the long chain substituents in **M5**. The range of surface pressure is only slightly larger for **M5** (0–9.5 mN m^{-1}) when compared with cryptophane **M** (0–3.5 mN m^{-1}; see Tables 1 and 2). This means that the interfacial film of **M5** is more stable than that obtained with **M**. However, a surface pressure of 9.5 mN m^{-1} is not significant in terms of stability. Another difference between **M** and **M5** is the partial recovery of the starting structure with **M5** during the decompression phase, which is not observed with **M**. We will see below that **M** and **M5** behave differently after 2 or more compression cycles.

Behavior of cryptophane M5 towards successive compression–decompression cycles

Three consecutive cycles applied to cryptophane **M5** are shown in Fig. 2. After one compression, the shape of the isotherm is strongly modified. The collapse pressure has disappeared and the $A^i_{\pi=0}$ value has decreased to about 1.25 nm^2 $molecule^{-1}$. The third and following π–A isotherms are almost identical. This is characteristic of a modification of the structure of the film at the air–water interface without recovering the initial assemblies during the decompression stage. This modification can be attributed to a degradation of the cryptophane molecule at the interface or to an association of the molecules through specific intermolecular interactions. The first hypothesis can be discarded, as the π–A isotherm is identical to the one depicted in Fig. 1 when the first diagram was recorded several hours after spreading **M5** onto the surface, proving that no chemical transformation occurred at the interface. Thus, we must conclude that during the first compression, the molecules of cryptophane **M5** develop some particular intermolecular interactions leading to a different kind of film. The interfacial film obtained after two compression–decompression cycles is much more stable, and a third cycle does not modify the profile of the isotherm anymore. Furthermore, the present film is also more stable under pressure and at 27 mN m^{-1} the pressure decreases by only 15% after 52 min. According to the compression curves and the $A^i_{\pi=0}$ value, the film is obviously more compact. During the first isotherm of **M5**, the K_s factor is in agreement with the formation of an expanded liquid phase (Table 2), the arrangement of the molecules at the air–water interface is not compact. For the subsequent isotherms, the K_s values are characteristic of a condensed liquid phase, the film is well organized.

Behavior of cryptophane M6 at the air–water interface

For cryptophane **M6** the diagram is located in the range of 2.20 to 0.80 nm^2 $molecule^{-1}$ and the π–A isotherm is significantly

Table 1 Surface pressure, π, and molecular area limits, A, of the compressibility domains of π–A isotherms for **M** and **M5**

	(I)		Plateau		(II)	
	π/mN m^{-1}	A/nm^2 $molecule^{-1}$	π/mN m^{-1}	A/nm^2 $molecule^{-1}$	π/mN m^{-1}	A/nm^2 $molecule^{-1}$
M	0–3.5	1.40–1.25	≈4	1.25–0.80	4–36	0.80–0.50
M5	0–9.5	2.00–1.60	≈10	1.60–1.05	10–40	1.05–0.50

Table 2 K_s maxima for successive isotherms of cryptophanes **M5** and **M6**

		A/nm^2 $molecule^{-1}$	Elasticity coefficient K_s/mN m^{-1}	π/mN m^{-1}
Cryptophane **M5**	First isotherm	1.68	55.9	5.4
	Second isotherm	1.05	158.3	11.4
	Third isotherm	1.05	158.1	11.8
Cryptophane **M6**	First isotherm	1.63	125	17.5
	Second isotherm	1.61	129	18.2

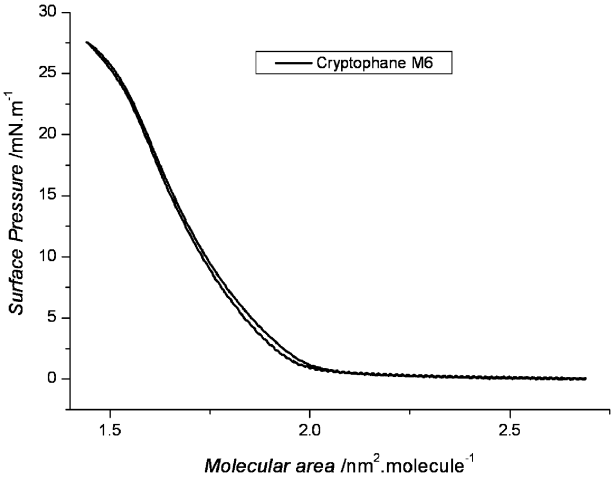

Fig. 3 π–A Reduced isotherm for a film of cryptophanes **M6**.

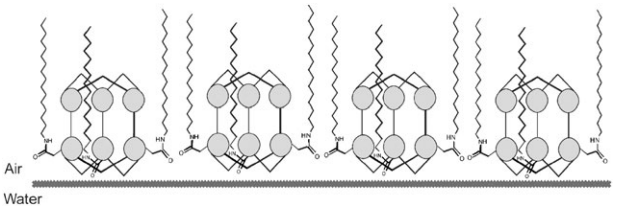

Scheme 3 Schematic representation of a monolayer of cryptophane **M6** at the air–water interface.

different from those observed with cryptophanes **M** and **M5**. A complete compression–decompression cycle until a surface pressure of 40 mN m^{-1} (Fig. 1), gives a π–A isotherm curve with three steps of compression and a strong hysteresis effect during the expansion stage, indicating the formation of irreversible 3D aggregates or condensed 2D phases with a low dispersion rate. The ascent (I) exists in an extended domain of surface pressure from 0 to 27 mN m^{-1}, for a molecular area in the range 2.00–1.50 nm^2 molecule^{-1}, followed by different zones of higher compressibility. This final part of the diagram for **M6**, from 1.50 to 0.80 nm^2 molecule^{-1}, presents some variations of the slope but no real plateau is observed. No modification occurred during three subsequent compression–decompression cycles. The lift-off area also located around 2 nm^2 molecule^{-1}, indicates similar behavior for both substituted molecules (**M5** and **M6**) at high surface areas. As for **M5**, the arrangement of cryptophane **M6** at the interface corresponds to a condensed liquid phase. The K_s value is lower than that measured with **M5** but both are the highest ones ever obtained with cryptophane molecules. The solid phase could not be observed, probably because of the large volume and the spherical shape of the molecule, which prevent compact arrangement at the interface. For **M6** a cycle limited to the first stage, compression until 27 mN m^{-1}, shows no hysteresis effect and introduces for the first time a 2D molecular arrangement that is perfectly reversible over a long range of surface pressure (Fig. 3). At 27 mN m^{-1}, no significant decrease of the surface pressure was observed after 1.5 h.

It thus appears that the introduction of long chain substituents, and especially three hydrophobic alkyl chains, leads to a real extension of the monolayer domain of the films of cryptophanes. The molecular area $A^i_{\pi=0}$ extrapolated at zero pressure, is roughly 2 nm^2 molecule^{-1} for **M5** and **M6**, and 1.40 nm^2 molecule^{-1} for **M**. Considering the 1.2–1.3 nm diameter of the cyclotriveratrylene unit (CTV), the surface occupied by a CTV at the air–water interface should be roughly 1.20–1.50 nm^2 molecule^{-1}. The $A^i_{\pi=0}$ determined for cryptophane **M** lies in this range, as its main section should correspond to the CTV area. Thus, the large difference observed with **M5** and **M6** can be attributed to the three peripheral hydrocarbon chains. By adding to the surface occupied by the spherical part of the host (about the one obtained for **M**), the molecular area corresponding to three hydrocarbon chains (0.20 nm^2 molecule^{-1} each), we obtain an $A^i_{\pi=0}$ value corresponding to that measured for **M5** and **M6**.

An interesting point concerns the structure of the films obtained with **M5** and **M6** and particularly the positioning of the host molecules at the water surface and the behavior of **M5** molecules in the compressed films. In cryptophane **M6**, the most polar parts of the molecule lie at the amide groups, which should be oriented towards the water surface, the long hydrophobic chains being directed to the air (Scheme 3). In such a description the film behaves at the interface as an ideal mixed film of cryptophanes and an amphiphilic lipid with the chains filling the voids between the spheres of cryptophanes (the cryptophane cavity can be roughly approximated as spheres). Since cryptophanes **M5** and **M6** have the same $A^i_{\pi=0}$ molecular area, **M5** films should present the same arrangement during the first compression. However, when the molecules are in contact, favorable interactions between two or more **M5** molecules appear and the molecules can overlap to form an apparent bilayer. Since this bilayer presents no real stability and no well-defined collapse pressure, we assume that the film is not well organized. This intermolecular rearrangement during the first compression step can be due to hydrogen bonding between the NHCO group of a molecule and the OH group of another molecule. This molecular aggregation takes place once the molecules are in contact and is strong enough to prevent their dissociation at the interface during the decompression step, so that their initial arrangement cannot be obtained anymore.

Conclusion

The precursor **M4** is a great improvement in the design of functionalized cryptophanes and offers a new route for the preparation of amphiphatic molecules. From **M4**, two new cryptophanes **M5** and **M6** have been synthesized, and other groups might be linked to **M4** in order to synthesize cryptophanes with targeted physical properties.

The monolayer domain of **M5** at the air–water interface only exists at small surface pressure (0–9.5 mN m^{-1}). After the first compression step, reorganization at the surface leads to the formation of an apparent bilayer. This behavior is certainly related to the formation of favorable intermolecular H-bonds when the molecules are in close contact. This supramolecular assembly of dimeric structures is stable enough to remain at the interface during the following compression–decompression stages. Unfortunately, anchoring to water is not strong enough and the bilayer is not well organized and therefore not stable enough to allow its transfer on a solid surface. Cryptophane **M6** reversibly forms the first really stable film of monomolecular thickness with a large domain of surface pressure 0–27 mN m^{-1}. Its compressibility factor is quite large (125 mN m^{-1}) and corresponds to a condensed liquid phase. The behavior of this film is quite remarkable and is the best one obtained so far with cryptophanes. This is attributed to favorable molecular interactions due to the long alkyl chain substituents of the cryptophane, which favor the organization of the molecules on the water subphase. At higher pressure both compounds form aggregates irreversibly.

Experimental

General

The ^{1}H NMR spectra were recorded at 200.13 MHz or 499.8 MHz on Bruker DPX200 and Varian Unity$^{\oplus}$ 500 spectrometers respectively. The ^{13}C NMR spectra were recorded at

50.3 MHz on a Bruker DPX200 spectrometer. ^{1}H and ^{13}C chemical shifts are expressed in ppm from TMS. ^{13}C assignments were mainly based on DEPT and 2D-correlation spectra. Elemental analyses and FAB mass spectra were performed by the Service Central d'Analyses, CNRS. Melting points were measured on a Reichert melting point apparatus or with a DSC7 Perkin Elmer microcalorimeter. Column chromatographic separations were carried out using Merck silica gel 60 (230–400 mesh). DMF was distilled from $MgSO_4$. Triestercyclotriveratrylene **1**[10] and brominated compound **3**[13]were synthesized according to literature procedures. Cryptophane **M** was synthesized as usual.[9]

Syntheses

(±)-2,7,12-Trihydroxy-3,8,13-tris(methoxycarbonylmethyl-thio)-10,15-dihydro-5*H*-tribenzo[*a*,*d*,*g*]cyclononene (2). A mixture of **1** (3 g, 4.46 mmol) and sodium isopropanethiolate (5 g, 50 mmol) in HMPA (20 mL) was stirred at 120 °C for 18 h. After cooling to room temperature, the solution was poured into 8N HCl (100 mL). A yellow precipitate was formed and recovered by filtration. The solid residue was washed with water and dichloromethane to discard a maximum amount of the sodium isopropanethiolate salt. The solid was then placed in 1,2-dichloroethane (100 mL) and methanol (50 mL), and concentrated sulfuric acid (1 mL) was added. The mixture was refluxed for 5 h. The organic phase was washed with a $NaHCO_3$ saturated aqueous solution and water until neutrality. The organic layer was dried over $MgSO_4$, filtered, and the solvent was evaporated under reduced pressure to give a solid, which was digested in diethyl ether to give 1.3 g (46%) of **2**, mp $>$ 226 °C (dec); ^{1}H NMR ($CDCl_3$): $\delta = 7.56$ (s, 3H, ArH), 7.43 (s, 3H, ArH), 6.97 (s, 3H, OH), 4.58 (d, 3H, $J = 13.5$ Hz, Ha), 3.68 (s, 9H, OCH_3), 3.57 (d, 3H, $J = 13.5$ Hz, He), 3.46 (d_{AB}, $J = 16.7$ Hz, SCH_2), 3.36 (d_{AB}, 3H, $J = 16.7$ Hz, SCH_2); ^{13}C NMR ($CDCl_3$): $\delta = 171.86$ (CO), 156.8, 143.85, 131.17, 116.84 (C_{aro}), 138.43, 116.94 (HC_{aro}), 53.06 (OCH_3), 39.29 (SCH_2), 36.01 ($ArCH_2$); elemental analysis calcd (%) for $C_{30}H_{30}O_9S_3 \cdot 0.5H_2O$ (639.76): C 56.32, H 4.88; found: C 56.49, H 4.90.

4-Tetrahydropyranoxymethyl-[(4-bromobutyl)oxy]-3-methoxybenzene (4). To a solution of **3** (22.9 g, 79 mmol) in CH_2Cl_2 (200 mL), were added dihydropyran (8.7 mL, 95 mmol) and paratoluenesulfonic acid (165 mg, 0,87 mmol). The mixture was stirred at room temperature for 2 h. The CH_2Cl_2 layer was washed with water until neutrality, dried over $MgSO_4$ and filtered. The solvent was evaporated under reduced pressure to afford compound **4** (29 g, 95%) as a colorless oil. ^{1}H NMR ($CDCl_3$): $\delta = 6.82$–6.88 (m, 3H, ArH), 4.68 (d_{AB}, 1H, $J = 11.8$ Hz, $ArCH_2O$), 4.65 (m, 1H, OCHO), 4.40 (d_{AB}, 1H, $J = 11.8$ Hz, $ArCH_2O$), 3.98 (t, 2H, $J = 5.9$ Hz, $ArOCH_2$), 3.84 (m, 1H, OCH_2), 3.83 (s, 3H, OCH_3), 3.48 (m, 1H, OCH_2), 3.43 (t, 2H, $J = 6.5$ Hz, CH_2Br), 1.51–2.01 (m, 10H, CH_2); ^{13}C NMR ($CDCl_3$): $\delta = 149.44$, 147.76, 131.12 (C_{aro}), 120.46, 113.08, 111.86 (HC_{aro}), 97.50 (OCO), 68.70, 68.86, 62.20 (OCH_2), 55.87 (OCH_3), 33.41 (CH_2Br), 30.55, 29.41, 27.80, 25.41, 19.42 (CH_2); elemental analysis calcd (%) for $C_{17}H_{25}O_4Br$ (373.29): C 54.70, H, 6.75; found: C 54.98, H 6.55.

2,7,12-Tris{4-[4-(tetrahydropyranoxymethyl)-2-methoxy-phenoxy]-butoxy}-3,8,13-tris(6-methoxycarbonylmethylthio)-10,15-dihydro-5*H*-tribenzo[*a*,*d*,*g*]cyclononene (5). To a solution of **2** (1.0 g, 1.6 mmol) and **4** (5.92 g, 15.9 mmol) in DMF (50 mL) was added 2.4 g of CsF (15.7 mmol). The reaction mixture was stirred at 50 °C under argon for 24 h. Then, more **4** (0.5 g, 1.34 mmol) and CsF (0.3 g, 1.97 mmol) were added and the mixture was further stirred for 24 h and then poured into cracked ice (300 mL). The mixture was extracted with CH_2Cl_2 (3 × 80 mL) and the combined organic phases were washed with water, dried over $MgSO_4$, filtered and the solvent was evaporated under vacuum. The oily residue was purified by column chromatography (CH_2Cl_2–EtOAc 9 : 1) to afford compound **5** (1.79 g, 75%) as a glassy solid. ^{1}H NMR ($CDCl_3$): $\delta = 7.36$ (s, 3H, ArH), 6.84–6.87 (m, 12H, ArH), 4.63 (d, 3H, $J = 13.5$ Hz, Ha), 4.69 (d, 3H, $J = 11.8$ Hz, $ArCH_2O$), 4.41 (d, 3H, $J = 11.8$ Hz, $ArCH_2O$), 4.07–4.15 (m, 12H, $ArOCH_2$), 3.83–3.85 (m, 3H, THP-OCH_2), 3.82 (s, 9H, OCH_3), 3.55 (s, 9H, CO_2CH_3), 3.57 (d_{AB}, 3H, $J = 13.1$ Hz, SCH_2), 3.50 (d_{AB}, 3H, $J = 13.1$ Hz, SCH_2), 3.59 (d, 3H, $J = 13.5$ Hz, He), 3.48–3.60 (m, 6H, THP-OCH_2 and OCHO), 2.0 (m, 12H, CH_2), 1.55–1.99 (br m, 18H, THP-CH_2); ^{13}C NMR ($CDCl_3$): δ 170.7 (CO), 156.29, 149.57, 148.19, 140.24 (OC_{aro} and SC_{aro}), 132.96, 121.44, 113.45, 113.11, 112.03 (HC_{aro}), 131.60, 131.01, 120.80 (C_{aro}), 97.75 (OCO), 69.01, 68.80, 68.30, 62.50 (OCH_2), 56.12 (OCH_3), 52.56 (CO_2CH_3), 36.60 ($ArCH_2$), 35.08 (SCH_2), 30.83, 26.27, 26.17, 25.69, 19.71 (CH_2); elemental analysis calcd (%) for $C_{81}H_{102}O_{21}S_3 \cdot H_2O$ (1525.89): C 63.76, H 6.87; found: C 63.85, H 6.83.

Cryptophane M4. A mixture of **5** (1 g, 66.5 mmol) in formic acid (600 mL) and $CHCl_3$ (30 mL) was stirred at 70 °C for 6 h. The resulting dark red solution was evaporated under vacuum. The residue was submitted to two cycles of dissolution–evaporation in chloroform (2 × 30 mL) to discard traces of formic acid. The residue was submitted to column chromatography (CH_2Cl_2–EtOAc 95 : 5) to give the desired cryptophane **M4** (0.23 g, 29%). ^{1}H NMR ($CDCl_3$): $\delta = 7.25$ (s, 3H, ArH), 6.80 (s, 3H, ArH), 6.79 (s, 3H, ArH), 6.65 (s, 3H, ArH), 4.59 (d_{AB}, 3H, $J = 13.6$ Hz, Ha), 4.55 (d_{AB}, 3H, $J = 13.6$ Hz, Ha), 4.28–4.10 (m, 6H, OCH_2), 3.75–3.86 (m, 6H, OCH_2), 3.71 (s, 9H, OCH_3), 3.69 (s, 9H, OCH_3), 3.63 (d_{AB}, 3H, $J = 14.8$ Hz, SCH_2), 3.47 (d, 3H, $J = 13.6$ Hz, He), 3.38 (d, 3H, $J = 13.6$ Hz, He), 3.36 (d_{AB}, 3H, $J = 14.8$ Hz, SCH_2), 1.94 (m, 12H, CH_2); ^{13}C NMR ($CDCl_3$): $\delta = 170.74$ (CO), 155.90, 148.72, 146.84, 140.04 (OC_{aro} and SC_{aro}), 132.68 (C_{aro}), 132.40 (HC_{aro}), 131.93, 131.68 (C_{aro}), 117.44, 114.90, 113.60 (HC_{aro}), 68.37, 67.32 (OCH_2), 56.13, 52.43 (OCH_3), 36.34 ($ArCH_2$), 35.14 (SCH_2), 24.74, 24.59 (CH_2); MS (FAB): m/z: 1201.3 $[M + H]^+$.

Cryptophane M5. A mixture of cryptophane **M4** (0.050 g, 0.04 mmol) and 6-aminohexan-1-ol (1 g, 8.5 mmol) was stirred under argon at 60 °C for 16 h. At this temperature the aminoalcohol melted. The residue was then dissolved in a minimum amount of CH_2Cl_2. An insoluble part containing some carbonated amine was filtered off and the solution was evaporated under vacuum. The residue was purified by column chromatography (CH_2Cl_2–MeOH 95 : 5) to give the cryptophane **M5** (0.46 g, 75%), mp 181 °C (dec). ^{1}H NMR ($CDCl_3$): $\delta = 6.95$ (s, 3H, ArH), 6.94 (m, 3H, NH–CO), 6.83 (s, 3H, ArH), 6.79 (s, 3H, ArH), 6.65 (s, 3H, ArH), 4.59 (d, 3H, $J = 14$ Hz, Ha), 4.35 (m, 3H, $ArOCH_2$), 4.17 (m, 3H, $ArOCH_2$), 3.85–3.80 (m, 6H, $ArOCH_2$), 3.68 (s, 9H, OCH_3), 3.57 (m, 6H, CH_2–OH), 3.53 (d_{AB}, 3H, $J = 17$ Hz, SCH_2), 3.39 (d, 3H, $J = 14$ Hz, He), 3.33 (m, 3H, CH_2–NH), 3.29 (d_{AB}, 3H, $J = 17$ Hz, SCH_2), 3.05–3.10 (m, 3H, CH_2–NH), 1.96 (m, 12H, CH_2), 1.24–1.28 (m, 6H, CH_2), 1.11–1.11 (m, 6H, CH_2); ^{13}C NMR ($CDCl_3$): $\delta = 168.4$ (CO), 155.0, 148.62, 146.22, 139.33 (OC_{aro} and SC_{aro}), 132.7, 132.6, 131.7, 122.1 (C_{aro}) 130.11, 117.3, 115.1, 113.5 (HC_{aro}), 68.3, 67.8 (OCH_2), 62.6 (CH_2–OH), 56.0 (OCH_3), 39.6 (CH_2–NH), 36.9 (SCH_2), 36.3, 36.16 ($ArCH_2$), 32.6, 29.4, 26.4, 25.4, 24.75 (CH_2); MS (FAB): m/z: 1456.8 $[M + H]^+$.

Cryptophane M6. A mixture of cryptophane **M4** (0.050 g, 0.04 mmol) and hexadecylamine (1 g, 4.1 mmol) in $CHCl_3$ (0.5 mL) was stirred under argon at 50 °C for 24 h. The cloudy mixture was totally homogeneous after 8 h. The residue was then purified by column chromatography (CH_2Cl_2–EtOAc, 90 : 10) to give the cryptophane **M6** (0.042 g, 55%). ^{1}H NMR

($CDCl_3$): $\delta = 6.95$ (s, 3H, ArH), 6.89–6.94 (m, 3H, NH), 6.80 (s, 6H, ArH), 6.65 (s, 3H, ArH), 4.60 (d_{AB}, 3H, $J = 14.2$ Hz, Ha), 4.52 (d_{AB}, 3H, $J = 14.2$ Hz, Ha), 4.29–4.31 (m, 3H, OCH_2), 4.12 –4.18 (m, 3H, OCH_2), 3.83–3.85 (m, 6H, OCH_2), 3.69 (s, 9H, OCH_3), 3.54 (d_{AB}, 3H, $J = 17.0$ Hz, SCH_2), 3.41 (d, 3H, $J = 13.6$ Hz, Ha), 3.39 (d, 3H, $J = 13.6$ Hz, He), 3.28 (d_{AB}, 3H, $J = 17.0$ Hz, SCH_2), 3.16–3.25 (m, 6H, CH_2N), 1.96 (m, 12H, CH_2), 1.24–1.48 (m, 84H, CH_2 chains), 0.85 (t, 9H, $J = 5.1$ Hz, CH_3); ^{13}C NMR ($CDCl_3$): $\delta = 168.3$ (CO), 155.00, 148.6, 146.9, 139.16 (OC_{aro} and SC_{aro}), 132.7, 132.4, 131.7, 122.3 (C_{aro}), 129.9, 117.4, 114.9, 113.6 (HC_{aro}), 68.5, 67.9 (OCH_2), 56.0 (OCH_3), 39.9 (NCH_2), 37.03 (SCH_2) 36.4 (2 $ArCH_2$), 31.9, 29.6, 29.5, 29.35, 26.8, 24.8, 22.7 (CH_2), 14.10 (CH_3); MS (FAB): m/z: 1829.3 $[M + H]^+$.

Langmuir setup and experimental procedure

The films were prepared on a thermostated home-made teflon Langmuir trough (51 × 13 cm) at 22.0 ± 0.2 °C. The cryptophanes were spread on the water surface from dichloromethane (distilled on $CaCl_2$) solutions of concentration 0.5 mmol dm^{-3}. The subphase was pure water purified by an automated ELGA System at a resistivity level of 18.2 MΩ. The desired amount of dichloromethane solution was delivered onto the water surface by means of a micro-syringe (Unimetrix), and the spreading was followed by a standby period of 20–30 min, allowing the evaporation of the solvent and the internal equilibrium of the expanded material to be settled.

Film compression and decompression were performed with a mobile barrier driven at a constant speed of 47 mm^2 s^{-1}. The surface pressure π, measured by the Wilhelmy method,[14] was continuously recorded during the barrier displacement, and the π–A isotherm diagrams were obtained after the usual standby period. For each cryptophane the initial molecular area extrapolated to zero pressure, $A^i_{\pi=0}$, was obtained by extrapolation of the π–A diagram of the first condensed phase observed during the compression process.

The stability of the cryptophane monolayers was checked by recording the evolution of the surface pressure at constant area for typical stages of compression. When necessary, standby periods of 3 h have been applied between two successive compression–decompression cycles in order to follow the specific evolution of the interfacial molecular organization *versus* time. The elasticity coefficient K_s, was identified by the dynamic dilatational modulus and defined as $K_s = A(\partial\pi/\partial A)_{T,P}$. It can be derived from the π–A isotherm diagrams and used to provide information on the cohesion of molecules in the interfacial film.

Acknowledgements

We thank G. Prevost for preliminary work. J.-C. Mulatier and M. Simon are acknowledged for skilful experimental contribution. Thanks are due to Dr A.W. Coleman for his interest in this work and further developments towards surface coatings with cryptophane molecules.

References

1 R. Zadmard, M. Arendt and T. Schrader, *J. Am. Chem. Soc.*, 2004, **126**, 7752–7753.
2 (*a*) M. Eddaoudi, A. Baszkin, H. Parrot-Lopez, M. Buissonnade and A. W. Coleman, *Langmuir*, 1995, **11**, 13–15; (*b*) M. T. Rojas, R. Königer, J. F. Stoddart and A. E. Kaifer, *J. Am. Chem. Soc.*, 1995, **117**, 336–343.
3 (*a*) M. D. Conner, V. Janout, I. Kudelka, J. Zhu and S. L. Regen, *Langmuir*, 1993, **9**, 2389–2397; (*b*) D. Vollhardt, J. Gloede, G. Weidemann and R. Rudert, *Langmuir*, 2003, **19**, 4228–4234; (*c*) A. Van der Heyden, J.-B. Regnouf-de-Vains, P. Warszyński, J.-O. Dalbavie, A. Żywociński and E. Rogalska, *Langmuir*, 2002, **18**, 8854–8861; (*d*) B.-H. Huisman, E. U. Thoden van Velzen, F. C. J. M. van Veggel, J. F. J. Engbersen and D. N. Reinhoudt, *Tetrahedron Lett.*, 1995, **36**(18), 3273–3276.
4 P. Prus, M. Pietraszkiewicz and R. Bilewicz, *Supramol. Chem.*, 1998, **10**, 17–25.
5 E. U. Thoden van Velzen, J. F. J. Engbersen and D. N. Reinhoudt, *Synthesis*, 1995, 989–997.
6 (*a*) A. Collet, *Tetrahedron*, 1987, **43**, 5725–5739; (*b*) A. Collet, J.-P. Dutasta, B. Lozach and J. Canceill, *Top. Curr. Chem.*, 1993, **165**, 103–129; (*c*) A. Collet, in *Comprehensive Supramolecular Chemistry*, ed. F. Vögtle, Pergamon, Oxford, 1996, vol. 2, pp. 325–365.
7 (*a*) J.-P. Chauvet, L. Gambut, A. Séauve, C. Garcia and A. Collet, *C. R. Acad. Sci., Ser II*, 1994, **318**, 771–776; (*b*) L. Gambut, J. P. Chauvet, C. Garcia, B. Berge, A. Renault, S. Rivière, J. Meunier and A. Collet, *Langmuir*, 1996, **12**, 5407–5412.
8 The cryptophane nomenclature is quite complicated and they are adequately named with a letter (then letter and number) in alphabetical order, which corresponds to the chronological order of their discovery (see ref. 6).
9 C. Garcia, A. Aubry and A. Collet, *Bull. Soc. Chim. Fr.*, 1996, **133**, 853–867.
10 (*a*) J. Costante, C. Garcia and A. Collet, *Chirality*, 1997, **9**, 446–453; (*b*) C. Garcia, C. Andraud and A. Collet, *Supramol. Chem.*, 1992, **1**, 31–45.
11 J. H. Clark, H. L. Holl and and J. M. Miller, *Tetrahedron Lett.*, 1976, **38**, 3361–3364.
12 L. G. Groenen, B. H. M. Ruël, A. Casnati, W. Verboon, A. Pochini, R. Ungaro and D. N. Reinhoudt, *Tetrahedron*, 1991, **39**, 8379–8384.
13 R. G Janssen, W. Verboom, J. P. M. Van Duynhoven, E. J. J. Van Verzen and D. N. Reinhoudt, *Tetrahedron Lett.*, 1994, **35**, 6555–6558.
14 A. W. Adamson, in *Physical Chemistry of Surfaces*, John Wiley and Sons, New York, 1982, p. 101.